

On the shifts of orbits and periodic orbits under perturbation and the change of Poincaré map Jacobian of periodic orbits

Wenyin Wei^{1,2,3}, Alexander Knieps³, and Yunfeng Liang^{1,3,*}

¹ *Institute of Plasma Physics, Hefei Institutes of Physical Science, Chinese Academy of Sciences, Hefei 230031, People's Republic of China*

² *University of Science and Technology of China, Hefei 230026, People's Republic of China and*

³ *Forschungszentrum Jülich GmbH, Institut für Energie- und Klimaforschung - Plasmaphysik, Jülich 52425, Germany*

(Dated: July 12, 2024)

Periodic orbits and cycles *resp.* play a significant role in discrete- and continuous-time dynamical systems (*i.e.* maps and flows). To succinctly describe their shifts when the system is applied perturbation, the notions of functional and functional derivative are borrowed from functional analysis to consider the whole system as an argument of the geometric representation of the periodic orbit or cycle. The shifts of an orbit/trajectory and periodic orbit/cycle are analyzed and concluded as formulae for maps/flows, respectively. The theory shall be beneficial to the sensitivity to perturbation analysis, control and optimization of various systems.

Introduction.— This paper develops a theory on the shifts of orbits and periodic orbits under perturbation, motivated by the practical need for three-dimensional (3D, *i.e.* non-axisymmetric) magnetic field design optimization and control in magnetically confined fusion (MCF) machines. However, the theory applies to arbitrary finite-dimensional dynamical systems (DSs) generated by ordinary differential equations (ODEs). Generalization to infinite-dimensional DSs [1] generated by partial differential equations (PDE) to offer a convenient computational method to estimate the sensitivity of the system to the initial conditions is possible but requires more effort beyond this Letter.

In the MCF community, the past practice [2–8], to mitigate or suppress Edge Localized Modes (ELMs) in tokamak plasmas involves introducing external Resonant Magnetic Perturbations (RMPs) to let island chains grow and corrode each other, then a chaotic field is created, also referred to as a stochastic field [9–11], owing to a lack of understanding of the long-term behaviour of field line tracing. It was expected that the chaotic field between island chains would reduce the transient heat flux released by ELMs by enhancing radial transport at the plasma edge. However, the theory underlying this practice has shortcomings due to relying on Fourier analysis of the radial magnetic perturbation $B^r = \mathbf{B} \cdot \nabla r$ in the flux coordinates (r, θ, φ) or its equivalents [12, 13] that require the integrability of the perturbed system. Although the term *stochastic field* is still widely used in the MCF community and Hamiltonian system-relevant research [14, 15], we advocate using the term *chaotic field* to avoid confusion, as researchers sometimes use chaotic and stochastic interchangeably in an attempt to obscure distinctions. The chaotic field expanded by the stable and unstable manifolds of the outermost X-cycle(s) is probably the largest one in MCF machines [16], prompting a return to the real-world cylindrical coordinates.

The chaotic field is not unique in toroidal magnetic fields but is common in autonomous continuous-time DSs

of three dimensions or more, not necessarily divergence-free. Chaos in 2D continuous-time DSs is forbidden by Poincaré-Bendixson theorem. For discrete-time DSs, one dimension is sufficient to allow chaos to exist.

Functional, a function of function, is not a novel concept introduced to physicists from mathematics. In quantum physics, it is a common practice to write various energy forms as functions of the electronic wave function ψ , which has established a systematical framework of density functional theory (DFT). The theory developed in this Letter considering the whole system as an argument of orbits and periodic orbits significantly enhances one's ability to analyze the change of these well-defined objects under perturbation to the system, which can be a bit more complicated than DFT due to the more complex composite relationships between functions.

Apart from MCF, this theory has a broad application range across numerous research domains concerned with the behaviour of a dynamical system [17–23] or the island-around-island hierarchy in the chaotic field [10, 24, 25]. For instance, in aircraft orbit optimization in aerospace dynamics [26–28], the propulsion force contributed by the engine can be treated as a kind of perturbation to the system. Then, when and in which direction to expel the exhaust gases in pursuit of the shortest time, the highest fuel efficiency, the heaviest load or the best trade-off among them become a problem that can be solved by leveraging this theory.

Deduction and demonstration.— For a N -dimensional dynamical (N -D) system and a 3D toroidal vector field in cylindrical coordinates as a special case of the former, as shown below,

$$\dot{\mathbf{x}} = \mathbf{B}(\mathbf{x}), \quad (1a)$$

$$\dot{\mathbf{x}}_{\text{pol}} = \frac{R\mathbf{B}_{\text{pol}}}{B_\phi}(\mathbf{x}_{\text{pol}}, \phi), \quad (1b)$$

write a trajectory as $\mathbf{X}(\mathbf{x}_0, t)$ and $\mathbf{X}(\mathbf{x}_{0,\text{pol}}, \phi_s, \phi_e)$, where \mathbf{x}_0 and $\mathbf{x}_{0,\text{pol}}$ are initial conditions, \mathbf{B}_{pol} and B_ϕ are poloidal and toroidal components of the field in standard

cylindrical coordinates, ϕ the azimuthal angle, ϕ_s and ϕ_e the starting and ending angles.

The theory is inspired by chaotic field-relevant research in the MCF community, so the deduction and results for these two forms are displayed together to facilitate the audience interested in either one utilizing them. One thing worth emphasizing is that the theory in this Letter does not require the field \mathbf{B} to be divergence-free, so it can be applied to general vector fields, *e.g.* fluid velocity and current density fields.

$$\frac{\partial}{\partial t} \mathcal{D}\mathbf{X} = \nabla \mathbf{B} \cdot \mathcal{D}\mathbf{X} \quad (2a)$$

$$\frac{\partial}{\partial \phi_e} \mathcal{D}\mathbf{X}_{\text{pol}} = \underbrace{\frac{\partial(R\mathbf{B}_{\text{pol}}/B_\phi)}{\partial(R, Z)}}_{\text{abbr. as } \mathbf{A}=\mathbf{A}(R, Z, \phi)} \cdot \mathcal{D}\mathbf{X}_{\text{pol}} \quad (2b)$$

where \mathcal{D} means the partial derivative *w.r.t.* \mathbf{x}_0 or $\mathbf{x}_{0,\text{pol}}$. Note that $\mathbf{A} = \mathbf{A}(R, Z, \phi)$ is a function of spatial coordinates directly, $\mathbf{X}_{\text{pol}}(\mathbf{x}_{0,\text{pol}}, \phi_s, \phi_e)$ is a function of the initial point (not *in-situ*). To emphasize the difference, two derivative operators $\partial/\partial(R, Z)$ and \mathcal{D} are used.

The term X-cycle is a figurative alias of *hyperbolic cycle* (see Fig. 1(a)). A cycle is *hyperbolic* if

$$|\lambda_i| \neq 1 \text{ for all eigenvalues of } \mathcal{D}\mathcal{P}^m,$$

or equiv. $|\lambda_i| \neq 1$ for all eigenvalues of $\mathcal{D}\mathbf{X}_T$ except

the one corresponding to the eigenvector $\mathbf{v}_i = \hat{\mathbf{b}}$, where $\hat{\mathbf{b}}$ is the column vector of the local field normalized. An O-cycle can be similarly defined in 3-D continuous-time systems with both $\mathcal{D}\mathcal{P}^m$ eigenvalues $\lambda_i \in \mathbb{S} \subset \mathbb{C}$ but $\neq \pm 1$. \mathcal{P} denotes the Poincaré map. For a 3D toroidal vector field, the Poincaré section is chosen to be, in this Letter, an R - Z cross-section, while m is the toroidal turn number of the cycle. For a general N -D system, \mathcal{P}^m can be defined as the returning map as a whole with no individual meaning of m . The evolution of $\mathcal{D}\mathcal{P}^m$ and $\mathcal{D}\mathbf{X}_T$ along a cycle has been revealed by two formulae given in [29]:

$$\frac{d}{dt} \mathcal{D}\mathbf{X}_T = [\nabla \mathbf{B}, \mathcal{D}\mathbf{X}_T] \quad (3a)$$

where $\mathcal{D}\mathbf{X}_T$ is short for the full-period Jacobian on the cycle, that is $\mathcal{D}\mathbf{X}(\mathbf{x}_0, T)|_{\mathbf{x}_0=\mathbf{X}(\mathbf{x}_{\text{fix}}, t)}$, \mathbf{x}_{fix} is a fixed point on the cycle, and

$$\frac{d}{d\phi} \mathcal{D}\mathcal{P}^m = \left[\frac{\partial(R\mathbf{B}_{\text{pol}}/B_\phi)}{\partial(R, Z)}, \mathcal{D}\mathcal{P}^m \right] = [\mathbf{A}, \mathcal{D}\mathcal{P}^m]. \quad (3b)$$

Partial and total functional derivatives are denoted by $\delta/\delta\mathcal{B}$ and $d/d\mathcal{B}$, but they are inconvenient to use due to their infinite-dimensional nature. So they are often accompanied with a given perturbation $\Delta\mathcal{B}$ to be directional derivatives as $\Delta\mathcal{B} \cdot \delta/\delta\mathcal{B}$ and $\Delta\mathcal{B} \cdot d/d\mathcal{B}$. In this Letter, when a function symbol is written in calligraphic font, it means that it is not evaluated for a specific value

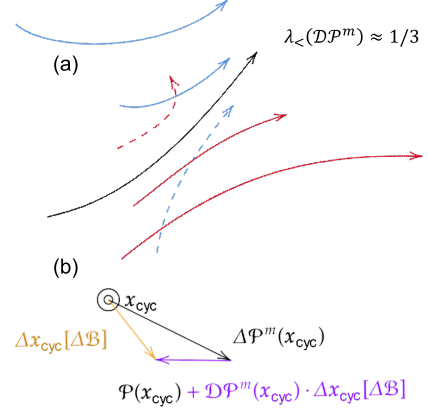


FIG. 1. (a) Cartoon to show the geometry meaning of $\mathcal{D}\mathcal{P}^m$ eigenvalues, (b) Cartoon to show how to calculate the shift of a fixed point for a map under perturbation.

but considered as a standalone object. The Poincaré map \mathcal{P} is a special case also written in calligraphic font but for not to be misunderstood as a vector field. An alternative notation of directional partial derivative equivalent to $\prod_k (\Delta \mathcal{B}_k \cdot \delta/\delta\mathcal{B}) \mathbf{X}$ is $\delta^k \mathbf{X}[\mathcal{B}; \Delta \mathcal{B}_1, \dots, \Delta \mathcal{B}_k]$ (see [30]), of which the argument list can be omitted for brevity.

With the whole system \mathcal{B} considered as an argument of \mathbf{X} , the equation (2a) becomes

$$\frac{\partial}{\partial t} \mathbf{X}[\mathcal{B}](\mathbf{x}_0, t) = \mathbf{B}(\mathbf{X}) = \mathbf{B}[\mathcal{B}](\mathbf{X}[\mathcal{B}](\mathbf{x}_0, t)). \quad (4)$$

Impose directional functional derivatives on both sides, then

$$\frac{\partial}{\partial t} \delta \mathbf{X}[\mathcal{B}; \Delta \mathcal{B}](\mathbf{x}_0, t) = \Delta \mathbf{B}[\mathcal{B}; \Delta \mathcal{B}](\mathbf{X}[\mathcal{B}](\mathbf{x}_0, t)) + \delta \mathbf{X}[\mathcal{B}; \Delta \mathcal{B}](\mathbf{x}_0, t) \cdot \nabla \mathbf{B} \quad (5)$$

Since the the perturbation $\Delta \mathcal{B}$ is usually a given one rather than a series of different perturbations ($\Delta \mathcal{B}_1, \Delta \mathcal{B}_2, \dots$), $\delta \mathbf{X}[\mathcal{B}; \Delta \mathcal{B}](t)$ can be concisely represented as $\delta \mathbf{X}$, similarly $\delta^2 \mathbf{X}[\mathcal{B}; \Delta \mathcal{B}, \Delta \mathcal{B}](t)$ as $\delta^2 \mathbf{X}$. With arguments omitted, the equation (5) becomes

$$\frac{\partial}{\partial t} \delta \mathbf{X} = \Delta \mathbf{B} + \delta \mathbf{X} \cdot \nabla \mathbf{B} \quad (6)$$

Similarly, for the second and third variations,

$$\frac{\partial}{\partial t} \delta^2 \mathbf{X} = 2(\delta \mathbf{X} \cdot \nabla) \Delta \mathbf{B} + \delta \mathbf{X} \delta \mathbf{X} : \nabla^2 \mathbf{B} + \delta^2 \mathbf{X} \cdot \nabla \mathbf{B}. \quad (7)$$

where the semicolon is defined as $\mathbf{a}\mathbf{b} : \mathbf{c}\mathbf{d} = (\mathbf{a} \cdot \mathbf{c})(\mathbf{b} \cdot \mathbf{d})$,

$$\begin{aligned} \frac{\partial}{\partial t} \delta^3 \mathbf{X} = & 3(\delta^2 \mathbf{X} \cdot \nabla) \Delta \mathbf{B} + 3(\delta \mathbf{X} \delta \mathbf{X} : \nabla^2) \Delta \mathbf{B} \\ & + 3\delta \mathbf{X} \delta^2 \mathbf{X} : \nabla^2 \mathbf{B} + \delta \mathbf{X} \delta \mathbf{X} \delta \mathbf{X} : \nabla^3 \mathbf{B} + \delta^3 \mathbf{X} \cdot \nabla \mathbf{B} \end{aligned} \quad (8)$$

The deduction can be continued to higher orders. The shift of a trajectory under perturbation to the whole system can be approximated by the following Taylor expansion based on these variations,

$$\mathbf{X}[\mathcal{B} + \Delta\mathcal{B}](\mathbf{x}_0, t) = \mathbf{X}[\mathcal{B}](\mathbf{x}_0, t) + \delta\mathbf{X} + \delta^2\mathbf{X}/2! + \dots + \delta^k\mathbf{X}/k! + \mathcal{O}(\|\Delta\mathcal{B}\|^{k+1}). \quad (9)$$

To migrate Eqs. (4-8) from flows to maps, *e.g.*

$$\mathbf{X}[\mathcal{B}](\mathbf{x}_0, n+1) = \mathcal{P}[\mathcal{P}](\mathbf{X}[\mathcal{B}](\mathbf{x}_0, n)), \quad (10)$$

where $\mathcal{P} : \mathbb{R}^N \rightarrow \mathbb{R}^N$ denotes a general map, one simply needs to replace $\partial\mathbf{X}/\partial t$ on the left hand side (LHS) with $\mathbf{X}(n+1)$, and \mathbf{X} on the right hand side (RHS) with $\mathbf{X}(n)$.

Equations (4-9) do not need to make substantial change if the system is non-autonomous, *i.e.* the time is an explicit variable of the field $\mathbf{B} = \mathbf{B}(t, \mathbf{x})$.

Thereafter, one can calculate the shifts of a periodic orbit and a cycle *resp.* based on the first variations $\delta\mathcal{P}^m$ and $\delta\mathbf{X}_T$ with the aid of $\mathcal{D}\mathcal{P}^m$, as explained in Fig. 1(b). Note that a periodic orbit and cycle are defined to be those the initial point of which is tied to the ending point. The idea to calculate the shift is \mathbf{x}_{cyc} must have such a shift $\Delta\mathbf{x}_{\text{cyc}}$ that the ending point $\mathcal{P}(\mathbf{x}_{\text{cyc}})$ after perturbation keeps matching the starting point, *i.e.*

$$\Delta\mathbf{x}_{\text{cyc}} = \Delta\mathcal{P}^m(\mathbf{x}_{\text{cyc}}) + \mathcal{D}\mathcal{P}^m(\mathbf{x}_{\text{cyc}}) \cdot \Delta\mathbf{x}_{\text{cyc}} + \dots, \quad (11)$$

$$\begin{aligned} \Delta\mathbf{x}_{\text{cyc}} &= [\mathcal{D}\mathcal{P}^m(\mathbf{x}_{\text{cyc}}) - \mathbf{I}]^{-1} \cdot [-\Delta\mathcal{P}^m(\mathbf{x}_{\text{cyc}})] \\ &= [\mathcal{D}\mathcal{P}^m(\mathbf{x}_{\text{cyc}}) - \mathbf{I}]^{-1} \cdot \end{aligned}$$

$$\left(-\delta\mathcal{P}^m[\mathcal{B}; \Delta\mathcal{B}](\mathbf{x}_{\text{cyc}}) + \mathcal{O}(\|\Delta\mathcal{B}\|^2) \right) + \dots, \quad (12)$$

$\delta\mathcal{P}^m$ on RHS contributes the first order variation, so

$$\delta\mathbf{x}_{\text{cyc}} = -[\mathcal{D}\mathcal{P}^m - \mathbf{I}]^{-1} \cdot \delta\mathcal{P}^m, \quad (13)$$

which applies to periodic orbits and cycles whose full-period Jacobians $\mathcal{D}\mathcal{P}^m$ do not have eigenvalues equal to one. For those on center manifolds, this condition is broken, requiring a different analysis. Deduction for higher-order $\delta^k\mathbf{x}_{\text{cyc}}$ is put in Supplemental Material [31].

To apply Eq. (13) to an N -D flow, one needs to define a local $(N-1)$ -D Poincaré plane for every point on the concerned cycle to define $\mathcal{D}\mathcal{P}^m$. A natural choice is the local plane perpendicular to the cycle. To avoid constructing a frame of coordinates on the plane, a suggested way is to utilize the relationship between $\mathcal{D}\mathbf{X}_T$ and the local Poincaré map Jacobian. The local Poincaré map Jacobian has the same eigenvalues λ_i as $\mathcal{D}\mathbf{X}_T$ but with eigenvectors projected to the Poincaré plane $\mathbf{v}_{i\perp} = \mathbf{v}_i - \hat{\mathbf{b}}\hat{\mathbf{b}}^T \cdot \mathbf{v}_i$. Decompose $\Delta\mathbf{x}_{\text{cyc}}$ to be the sum of eigenvectors as $\Delta\mathbf{x}_{\text{cyc}} = \delta_{\perp}\mathbf{x}_{\text{cyc}} = \sum c_i \mathbf{v}_{i\perp}$. Then one can replace $\mathcal{D}\mathcal{P}^m(\mathbf{x}_{\text{cyc}}) \cdot \Delta\mathbf{x}_{\text{cyc}}$ in Eq. (11) with $\sum c_i \lambda_i \mathbf{v}_{i\perp}$. The first variation for $\Delta\mathcal{P}^m(\mathbf{x}_{\text{cyc}})$ is $\delta_{\perp}\mathbf{X}_T := \delta\mathbf{X}_T - \hat{\mathbf{b}}\hat{\mathbf{b}}^T \cdot \delta\mathbf{X}_T$. Then one can solve for the coefficients c_i to determine

$\delta_{\perp}\mathbf{x}_{\text{cyc}}$. The other way is to reuse the definition, keeping the starting and ending points tied to solve for the shift, but this time take into account projecting $\delta\mathbf{X}_T$ and $\mathcal{D}\mathbf{X}_T \cdot \delta_{\perp}\mathbf{x}_{\text{cyc}}$ to the perpendicular Poincaré plane,

$$\delta_{\perp}\mathbf{x}_{\text{cyc}} = (\mathbf{I} - \hat{\mathbf{b}}\hat{\mathbf{b}}^T) \cdot \delta\mathbf{X}_T + (\mathbf{I} - \hat{\mathbf{b}}\hat{\mathbf{b}}^T) \cdot \mathcal{D}\mathbf{X}_T \cdot \delta_{\perp}\mathbf{x}_{\text{cyc}}, \quad (14)$$

of which the LHS is the starting point shift, while RHS is the ending point shift consists of two terms: the first one is contributed by the perturbation and the second one is propagated from the starting point shift via $\mathcal{D}\mathbf{X}_T$. Reorganize Eq (14) to be

$$\delta_{\perp}\mathbf{x}_{\text{cyc}} = \left[\mathbf{I} - (\mathbf{I} - \hat{\mathbf{b}}\hat{\mathbf{b}}^T) \cdot \mathcal{D}\mathbf{X}_T \right]^{-1} \cdot (\mathbf{I} - \hat{\mathbf{b}}\hat{\mathbf{b}}^T) \cdot \delta\mathbf{X}_T. \quad (15)$$

To avoid repetitive calculation of $\delta\mathbf{X}_T$ and $\delta\mathcal{P}^m$ for every point on the cycle, their evolution along the cycle is concluded as the following formulae,

$$\frac{d}{dt}\delta\mathbf{X}_T = \mathbf{A} \delta\mathbf{X}_T - (\mathcal{D}\mathbf{X}_T - \mathbf{I})\Delta\mathbf{B}, \quad (16a)$$

$$\frac{d}{dt}\delta\mathcal{P}^m = \mathbf{A} \delta\mathcal{P}^m - (\mathcal{D}\mathcal{P}^m - \mathbf{I})\Delta\frac{R\mathbf{B}_{\text{pol}}}{B_{\phi}}, \quad (16b)$$

where $\Delta(R\mathbf{B}_{\text{pol}}/B_{\phi})$ is short for $(\Delta\mathcal{B} \cdot d/d\mathcal{B})(R\mathbf{B}_{\text{pol}}/B_{\phi})$, that is $\left(R\Delta\mathbf{B}_{\text{pol}}/B_{\phi} - R\Delta\mathbf{B}_{\text{pol}}/B_{\phi}^2 \cdot \Delta B_{\phi} \right)$.

The calculation of $\Delta\mathbf{x}_{\text{cyc}}$ given by Eq. (13) is just for one cross-section. To acquire $\Delta\mathbf{x}_{\text{cyc}}$ for all cross sections, the formula governing its evolution along a cycle in cylindrical is concluded as below (17b)

$$\frac{d}{d\phi}\delta_{\perp}\mathbf{x}_{\text{cyc}} \equiv \mathbf{A} \cdot \delta_{\perp}\mathbf{x}_{\text{cyc}} + \Delta\mathbf{B}, \quad (17a)$$

$$\frac{d}{d\phi}\delta\mathbf{x}_{\text{cyc}} = \mathbf{A} \cdot \delta\mathbf{x}_{\text{cyc}} + \Delta\frac{R\mathbf{B}_{\text{pol}}}{B_{\phi}}. \quad (17b)$$

A concise expression like Eq. (17a) for $d/d\phi \delta_{\perp}\mathbf{x}_{\text{cyc}}$ in an N -D flow as a counterpart of Eq. (17b) has not been found. What the authors deduced is too verbose to be a formula, of which the main complexity comes from the fact that $\hat{\mathbf{b}}$ changes along the cycle so the equation involves $\mathbf{B} \cdot \nabla\hat{\mathbf{b}}$ and becomes difficult to reduce.

Hereafter, the full-period Jacobian on a cycle and its change under perturbation will be examined. As a first step, with the whole system \mathcal{B} considered as an argument, the equation $\partial_{\phi_e}\mathcal{D}\mathbf{X}_{\text{pol}}(\mathbf{x}_{0,\text{pol}}, \phi_s, \phi_e) = \mathbf{A} \mathcal{D}\mathbf{X}_{\text{pol}}$ (2b) is complicated into

$$\begin{aligned} &\frac{\partial}{\partial\phi_e}\mathcal{D}\mathbf{X}_{\text{pol}}[\mathcal{B}](\mathbf{x}_{\text{cyc}}[\mathcal{B}])(\phi_s, \phi_s, \phi_e) \\ &= \mathbf{A}[\mathcal{B}](\mathbf{x}_{\text{cyc}}[\mathcal{B}])(\phi_e, \phi_e) \mathcal{D}\mathbf{X}_{\text{pol}}[\mathcal{B}](\mathbf{x}_{\text{cyc}}[\mathcal{B}])(\phi_s, \phi_s, \phi_e), \end{aligned} \quad (18)$$

of which an integration in ϕ_e after imposed $\Delta\mathcal{B} \cdot \frac{d}{d\mathcal{B}}\mathcal{B}$ gives $(\Delta\mathcal{B} \cdot \frac{d}{d\mathcal{B}})\mathcal{D}\mathbf{X}_{\text{pol}}$ on LHS. Note that this is a total derivative considering the influence from the \mathbf{x}_{cyc} shift. Writing it as $\delta\mathcal{D}\mathbf{X}_{\text{pol}}$ will mislead readers to think it is a

partial derivative without changing its starting point position, so it is not suggested. The \mathcal{DP}^m evolution formula $d/d\phi \mathcal{DP}^m = [\mathbf{A}, \mathcal{DP}^m]$ (2a) can be similarly processed, which yields $(\Delta\mathcal{B} \cdot \frac{d}{d\mathcal{B}})\mathcal{DP}^m$ on all sections. The relevant deduction is put in Supplemental Material [31].

By the \mathcal{DP}^m evolution formula, the \mathcal{DP}^m of X-cycles at the edge island chain in the standard configuration of Wendelstein 7-X at all ϕ -sections have been calculated and shown in Fig. 2 by the eigenvectors. Let the vacuum field of the upper control coils be the perturbation $\mathcal{B} = \mathcal{B}_{\text{std}} + k\Delta\mathcal{B}_{\text{pert}}$. The calculated $(\Delta\mathcal{B} \cdot \frac{d}{d\mathcal{B}})\mathcal{DP}^m$ has been verified by results acquired in a brute-force way (that is, simply relocate the X-cycle and recalculate \mathcal{DP}^m), as shown in Fig. 3(c). In Fig. 3(c), the eigenvectors of \mathcal{DP}^m at different k are drawn as ribbons to present the change tendency vividly. The yellow dashed edges corresponding to the $(1 + \Delta\mathcal{B} \cdot \frac{d}{d\mathcal{B}})\mathcal{DP}^m$ match the black edge lines corresponding to $k = 1$ as expected.

Not only can one employ the theory to fix an X-cycle at the designed position in the divertor region, but also to keep the eigenvalues of \mathcal{DP}^m close to unity (for longer field line connection lengths to ease detachment) during operation to resist the possibly opposite influences imposed by the plasma response field [32–35].

Conclusion and discussion.— A theory on the shifts of orbits/trajectories and periodic orbits/cycles has been developed, providing a deeper understanding of the nature of chaotic fields. This understanding allows fusion machines to move beyond relying solely on plasma diffusion to increase the power decay length λ_q of the scrape-off layer [36]. Instead, a proactive stimulation of chaotic fields can be employed to disperse heat flux in midair before it reaches the target plate. Moreover, this theory has implications beyond fusion research, offering insights into the behaviour and sensitivity to perturbation of complex systems in various domains. Agile and accurate prediction of orbit and periodic orbit shifts under perturbation can guide practitioners in quickly identifying the desired perturbation to the system.

This work has been carried out within the framework of the EUROfusion Consortium, funded by the European Union via the Euratom Research and Training Programme (Grant Agreement No 101052200 –EUROfusion). Views and opinions expressed are however those of the author(s) only and do not necessarily reflect those of the European Union or the European Commission. Neither the European Union nor the European Commission can be held responsible for them.

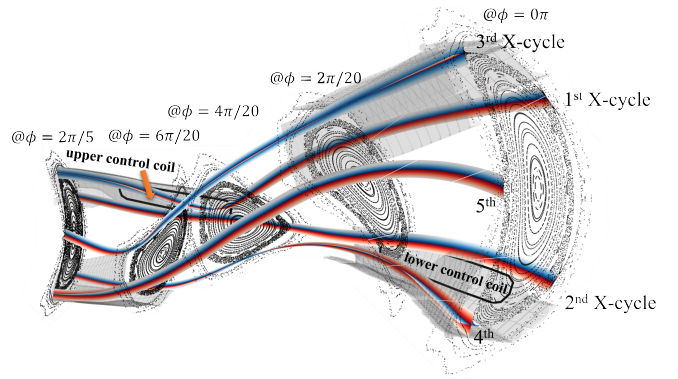


FIG. 2. Five typical Poincaré plots for Wendelstein 7-X standard configuration. Red and blue ribbons *resp.* indicate the directions of \mathcal{DP}^1 ($m = 1$) unstable and stable eigenvectors corresponding to $\lambda_i = 1.94965374$ and 0.51291252 .

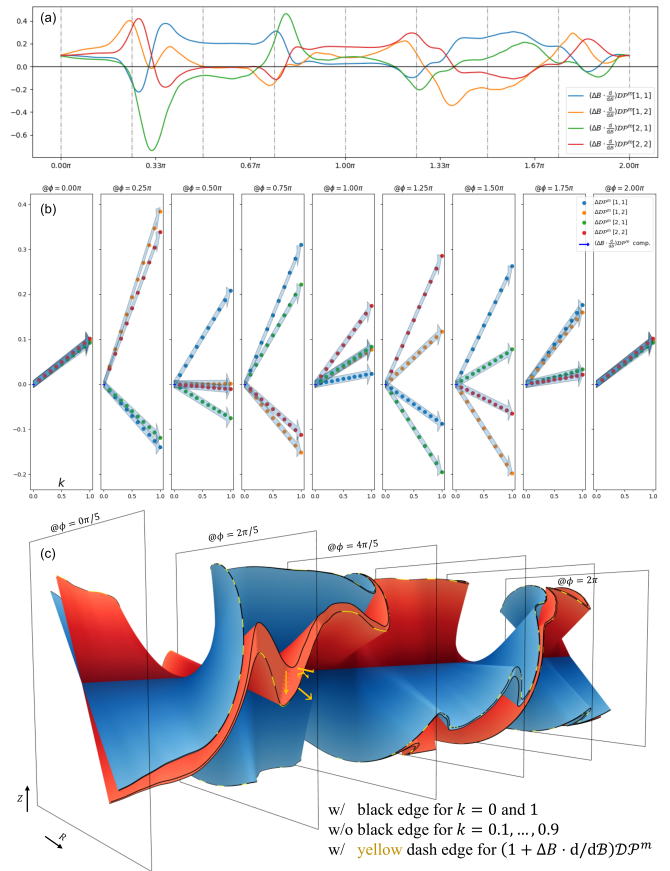


FIG. 3. The change of \mathcal{DP}^m of the first X-cycle at the edge $\nu = n/m = 5/5$ island chain of Wendelstein 7-X standard configuration. $(\Delta\mathcal{B} \cdot d/d\mathcal{B})\mathcal{DP}^m$ components are shown in (a) and as transparent blue arrows in (b). Scatter points show the reference values for the changes of \mathcal{DP}^m components computed for each k . (c) \mathcal{DP}^m eigenvectors against ϕ .

* y.liang@fz-juelich.de

- [1] R. Rudnicki, Math. Meth. Appl. Sci. **27**, 723 (2004).
- [2] Y. Liang *et al.*, Phys. Rev. Lett. **98**, 265004 (2007).
- [3] Y. Liang *et al.*, Phys. Rev. Lett. **105**, 065001 (2010).

- [4] Y. Liang *et al.*, Phys. Rev. Lett. **110**, 235002 (2013).
- [5] H. Frerichs *et al.*, Phys. Rev. Lett. **125**, 155001 (2020).
- [6] R. K. W. Roeder *et al.*, Phys. Plasmas **10**, 3796 (2003).
- [7] T. E. Evans *et al.*, Phys. Plasmas **9**, 4957 (2002).
- [8] T. E. Evans *et al.*, J. Phys.: Conf. Ser. **7**, 174 (2005).
- [9] S. S. Abdullaev *et al.*, J. Plasma Phys. **81**, 475810501 (2015).
- [10] S. Abdullaev, *Magnetic Stochasticity in Magnetically Confined Fusion Plasmas: Chaos of Field Lines and Charged Particle Dynamics*, Springer Series on Atomic, Optical, and Plasma Physics (Springer International Publishing, 2016).
- [11] J. E. Howard *et al.*, Phys. Rev. A **29**, 418 (1984).
- [12] R. Balescu *et al.*, Phys. Rev. E **58**, 951 (1998).
- [13] R. Balescu, Phys. Rev. E **58**, 3781 (1998).
- [14] B. Unterberg, Nucl. Fusion **50**, 030201 (2010).
- [15] R. S. MacKay *et al.*, Phys. Rev. Lett. **52**, 697 (1984).
- [16] H. Frerichs *et al.*, Phys. Plasmas **22**, 072508 (2015).
- [17] M. Harsoula *et al.*, Phys. Rev. E **97**, 022215 (2018).
- [18] J. D. Meiss, Chaos **25**, 097602 (2015).
- [19] E. E. Zotos, Nonlinear Dyn. **79**, 1665 (2015).
- [20] H. T. Moges *et al.*, Physica D **431**, 133120 (2022).
- [21] M. V. Falessi *et al.*, J. Plasma Phys. **81**, 495810505 (2015).
- [22] G. Di Giannatale *et al.*, Phys. Plasmas **25**, 052306 (2018).
- [23] F. Pegoraro *et al.*, Plasma Phys. Control. Fusion **61**, 044003 (2019).
- [24] J. D. Meiss, Phys. Rev. A **34**, 2375 (1986).
- [25] O. Alus *et al.*, Phys. Rev. E **90**, 062923 (2014).
- [26] A. F. Haapala and K. C. Howell, Int. J. Bifurcat. Chaos **26**, 1630013 (2016).
- [27] E. Trélat, Optim. Theory Appl. **154**, 712 (2012).
- [28] R. Chai *et al.*, Prog. Aerosp. Sci. **109**, 100543 (2019).
- [29] W. Wei *et al.*, Plasma Sci. Technol. **25**, 095105 (2023).
- [30] B. A. Frigiyik, S. Srivastava, and M. R. Gupta, *An Introduction to Functional Derivatives*, Tech. Rep. UWEETR-2008-0001 (Department of Electrical Engineering, University of Washington, Seattle, WA, USA, 2008).
- [31] See Supplemental Material at URL-will-be-inserted-by-publisher for the data for the deduction.
- [32] S. R. Hudson *et al.*, Phys. Rev. Lett. **89**, 275003 (2002).
- [33] J. Loizu *et al.*, J. Plasma Phys. **83**, 715830601 (2017).
- [34] S. Zhou *et al.*, Nucl. Fusion **62**, 106002 (2022).
- [35] A. Knieps *et al.*, Nucl. Fusion **62**, 026011 (2021).
- [36] T. Eich *et al.*, Phys. Rev. Lett. **107**, 215001 (2011).